Towards the understanding of the interaction effects between reflector antennas and phased array feeds

(article starts on next page)

Towards the Understanding of the Interaction Effects Between Reflector Antennas and Phased Array Feeds

O. A. Iupikov* R. Maaskant† M. Ivashina‡

Abstract — **A computationally efficient numerical procedure has been developed and used to analyze the mutual interaction effects between an electrically large reflector antenna and a phased array feed (PAF). The complex electromagnetic behavior for such PAF systems is studied through a few simple and didactical examples, among which a single dipole antenna feed, a singly-excited antenna in an array of 20 dipoles, and a fully-excited array. These examples account for the effects of the ground plane, active loading (low noise amplifiers), and beamforming scenario, and are used to illustrate the differences between single-port feeds and PAFs.**

1 INTRODUCTION

For many practical applications it is required to accurately model the beam patterns of reflector antennas. Several factors can cause the actual beam to differ from the ideally designed one due to inaccuracies of the antenna system model. For instance, one often neglects – or only partly takes into account – the effects of the feed supporting structure and reflector-feed interactions. A rigorous analysis of such electrically large antenna structures represents a challenging electromagnetic problem, especially when the reflector is fed with a phased array feed (PAF) consisting of many strongly coupled antenna elements. During the last few years a number of pioneering studies have been carried out towards the development of more complete numerical models [1–4] while, at the same time, knowledge has been acquired through experimental studies [5, 6]. For example, in [6] it has been observed that the magnitude of the receiving sensitivity ripple as a function of frequency caused by the feed-reflector interactions is significantly smaller for a PAF of wideband Vivaldi antennas than it is for a horn feed. It has been suggested that the smaller radar cross section (RCS) of Vivaldi PAFs is a reason for this improvement. However, the fact that there exist differences in the EM coupling mechanisms for different phased-array and single-element feeds, and how this affects the system design procedure, is not yet fully understood. The objective of the present work is therefore to investigate this phenomenon in more detail.

2 ANALYSIS METHODOLOGY

First, we examine a single dipole antenna feed above a finite ground plane, after which an array of dipole elements is considered, as shown in Fig. 1(a) and (b), respectively. The antenna array ports are connected to Low Noise Amplifiers (LNAs) which are also part of the antenna-receiver model. Two beamforming scenarios are considered: (i) a singly-excited embedded element, and; (ii) a fully-excited antenna array employing the Conjugate Field Matching (CFM) beamformer for maximizing the gain of the secondary far-field beam. This beamforming array system is analyzed in combination with a parabolic reflector of 8 m in diameter ($\sim 38\lambda$ @ $f = 1.42$ GHz), $F/D = 0.35$.

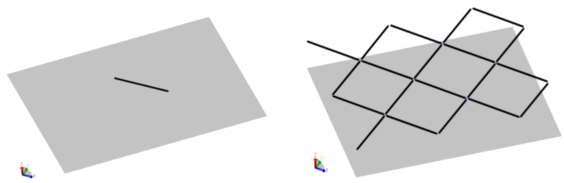

(a) (b)

Figure 1: The considered dipole antenna feeds: (a) a single dipole; and (b) a dual-polarized array of 20 dipole antenna elements. The dipole length is (0.47λ) and the ground plane size is $(3.3\lambda \times 2.65\lambda)$

To account for the mutual coupling between the feed and reflector antenna in the described system, a rapidly converging iterative procedure has been developed. It consists of the following steps: (i) the antenna feed currents are computed through a method-of-moments (MoM) approach by exciting the antenna port(s) in the absence of the reflector; (ii) these currents generate an EM field which induces PO-currents on the reflector surface; (iii) the PO currents create a scattered field that, in turn, induces currents on the feed structure. The steps (ii) and (iii) are repeated until the multiply induced currents – which form the total current when summed – has converged. Afterwards, the antenna

*Chalmers University of Technology, Dept. of Signals and Systems, 412 96, Gothenburg , Sweden, e-mail: oleg.iupikov@chalmers.se

†Chalmers University of Technology, Dept. of Signals and Systems, 412 96, Gothenburg , Sweden, e-mail: rob.maaskant@chalmers.se

‡Chalmers University of Technology, Dept. of Signals and Systems, 412 96, Gothenburg , Sweden, e-mail: marianna.ivashina@chalmers.se

radiation pattern, the input impedance (matrix) and derived antenna parameters affecting the receiving sensitivity can be computed.

It is worthwhile to mention that the antenna elements in our study are loaded by LNAs, so that we will account for this loading when solving for the antenna feed currents through the MoM. This is done through the modification of the diagonal elements of the MoM matrix corresponding to the port basis functions as described in [7, p. 223]. The impedance of the loads, and thus the input impedance of the LNAs, has been chosen real-valued. Next, the (passive) reflection coefficient of the antenna was minimized, which yielded the optimum load resistance of 80 and 140 Ω for the single dipole and array case, respectively.

To quantify the performance degradation of the antenna system – due to the interaction effects – we analyze the antenna efficiencies as well as the system noise temperature contributions, both of which affect the receiving sensitivity $A_{\text{eff}}/T_{\text{sys}}$ [8], i.e.,

$$\frac{A_{\text{eff}}}{T_{\text{sys}}} = \frac{A_{\text{ph}}\eta_{\text{ap}}\eta_{\text{rad}}}{\eta_{\text{rad}}T_{\text{spil}} + (1-\eta_{\text{rad}})\,T_{\text{amb}} + T_{\text{Eq}}^{\text{LNA}}} \tag{1}$$

where A_{ph} and A_{eff} are the physical and effective areas of the reflector antenna, respectively; T_{sys} – the system noise temperature; η_{ap} – the aperture efficiency; T_{spil} – the spillover noise temperature contribution; η_{rad} – the antenna radiation efficiency (herein assumed 100%); $T_{\text{amb}} = 290\text{K}$ – the ambient temperature; $T_{\text{Eq}}^{\text{LNA}}$ – the receiver noise temperature due to LNAs with minimum noise temperature T_{min}, a component which is independent from the antenna, and the noise coupling component T_{coup}, due to the impedance noise mismatch between the LNAs and the antenna elements [8].

In the next section it will be shown which of the above contributions are most affected by the feed-reflector interaction effects.

3 NUMERICAL RESULTS

The frequency-varying receiving sensitivity, which is caused by the interaction effects, gives rise to a standing wave component between feed and reflector with oscillation period $\Delta f = 2F/c$, where c is the speed of light [3]. Fig. 2 presents the computed current distributions on the ground plane of the three feeds at two frequency points leading to the minimum and maximum antenna aperture efficiency within one period of the oscillation. For the case of the single dipole [see Fig. 2(a)], one can clearly see a significant difference between the areas supporting large currents on the ground plane at these frequencies, as a result of which the corresponding far-field patterns of the feed differ in shape and beamwidth [see Fig. 3(a)].

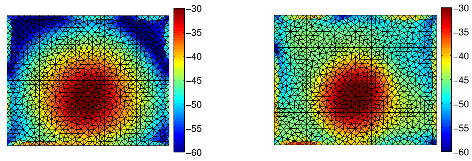

(a) Isolated dipole

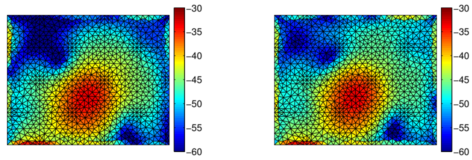

(b) Embedded dipole

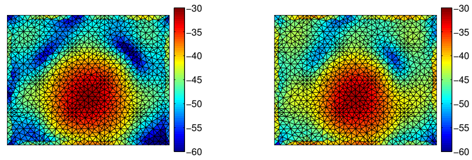

(c) Fully-excited array (CFM)

Figure 2: Current distributions on the ground plane of the feeds for two frequency points corresponding to the minimum (left column) and maximum (right column) of the aperture efficiency.

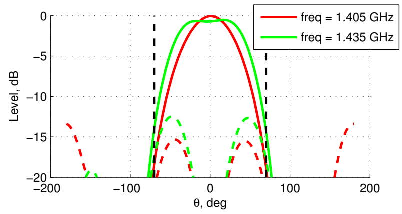

(a) Isolated dipole

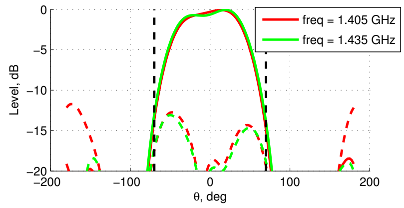

(b) Embedded dipole

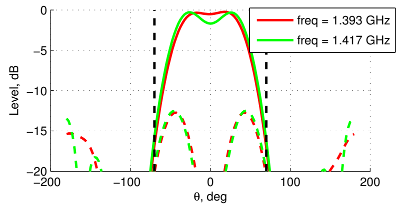

(c) Fully-excited array (CFM)

Figure 3: Primary patterns in $\phi = 45^\circ$ cross-section.

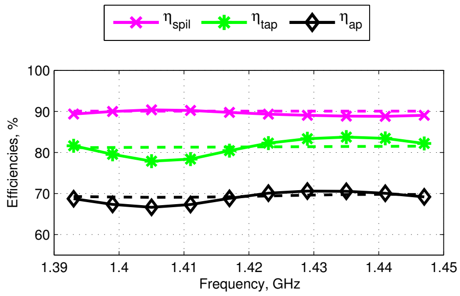

(a) Isolated dipole

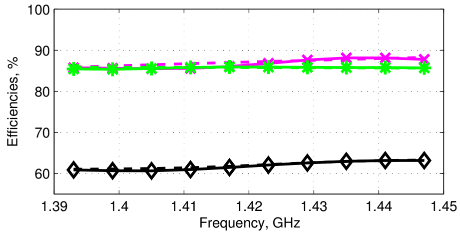

(b) Embedded dipole

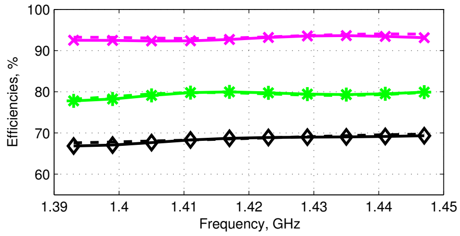

(c) Fully-excited array (CFM)

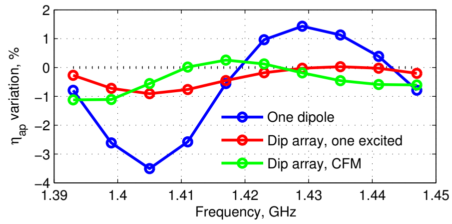

(d) Comparison of the η_{ap} variation

Figure 4: The aperture efficiency and its dominant contributions. The solid and dotted lines are for with and without accounting for feed-reflector interactions, respectively.

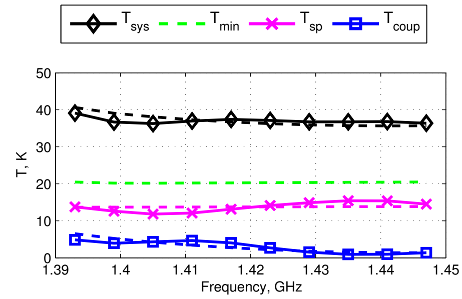

(a) Isolated dipole

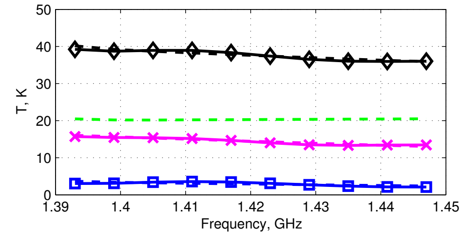

(b) Embedded dipole

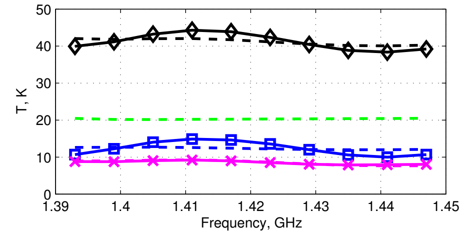

(c) Fully-excited array (CFM)

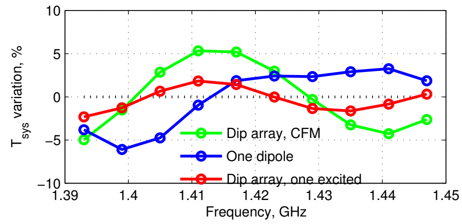

(d) Comparison of the T_{sys} variation

Figure 5: System noise temperature and its dominant contributions.

Upon comparing the left- and right-hand-side subfigures in Fig. 2, one observes that the ground-plane for the single-dipole case has a predominant effect on the scattering mechanism. On the contrary, when the field from the reflector illuminates the antenna array (the physical area of which is comparable to the size of the ground plane), part of this field is blocked by the dipoles. Therefore, the differences between the feed patterns for the dipole arrays in Fig. 3(b) and (c) are less pronounced, regardless of the beamforming scenario.

Next, we present the results for the system sensitivity and its subefficiencies for the three considered antenna feeds.

Fig. 4(a)–(c) shows the aperture efficiency and its dominant contributions, i.e., the spillover efficiency η_{spil} and the taper illumination efficiency η_{tap}; and Fig. 4(d) compares the respective frequency variations of η_{ap} due to the standing wave phenomenon. It is readily seen that the aperture efficiency variation is less than 1% for the two PAF cases, since the illumination pattern remains almost constant, whereas this variation is approximately three times larger for the single dipole case, due to the scattering mechanism differences as described above.

A similar analysis has been performed for the system noise temperature T_{sys} (see Fig. 5). Note that, for the embedded element case, T_{sys} is not affected much by the standing wave phenomenon, since the input impedance of a centralized dipole array element varies only little with frequency and is therefore well-matched (after optimally loading the array elements), as opposed to the single dipole antenna. Also, when beamforming is performed, the input impedance of each antenna array element (scan impedance) will differ from its optimal noise-match impedance, and therefore becomes more sensitive to the feed-reflector coupling. This results to higher T_{coup} and a stronger frequency variation. Hence, and in contrast to the systems employing single antenna feeds, the noise temperature due to mismatch effects, T_{coup}, is the dominant contribution to T_{sys} in case of PAF systems.

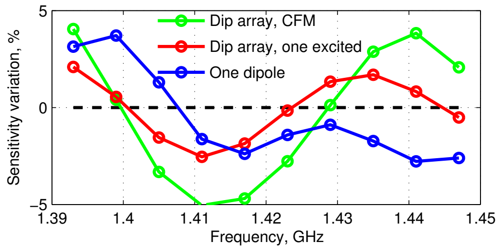

Figure 6: System sensitivity variation.

The sensitivity variation for all three cases is shown in Fig. 6. Although both η_{ap} and T_{sys} vary significantly for the system with a single dipole (i.e. -4% to 1.5%; and -5.5% to 3%, respectively), they partly compensate each other, leading to approximately the same sensitivity variation for all three feeding schemes.

4 CONCLUSIONS

The electromagnetic coupling between the reflector antenna and a single dipole feed was found to have a significant effect on the antenna beam shape and aperture efficiency, as opposed to the dipole PAFs. Our study indicates that the finite ground plane behind the single dipole, which is part of the feed supporting structure and often much larger than one antenna element, but comparable to the size of a PAF, is a reason for this difference. However, the (active) impedance matching of the strongly-coupled PAF elements appears to be more sensitive to the feed-reflector interaction, which has an impact on the receiver noise temperature. Similar conclusions were drawn from the numerical analysis of the checkerboard PAF of patch antennas [4], whereas these effects were found to be much smaller for the larger experimentally characterized array of 121 tapered-slot antenna elements [6]. The latter difference will be examined in more detail in future studies.

References

[1] N.-T. Huang, R. Mittra, M. Ivashina, and R. Maaskant, "Numerical study of a dual-polarized focal plane array (FPA) with vivaldi elements in the vicinity of a large feed box using the parallelized FDTD code GEMS," in *Proc. IEEE AP-S International Symposium*, Charleston, South Carolina, Jun. 2009, pp. 1–4.

[2] C. Craeye, "Analysis of complex phased array feeds and their interaction with a cylindrical reflector," in *Proc. IEEE AP-S International Symposium*, San Diego, California, Jul. 2008, pp. 1–4.

[3] M. A. Apeldoorn. (2011) M.sc. thesis: Characterizing reflector-feed interaction for parabolic reflector antennas. [Online]. Available: http://repository.tudelft.nl/view/ir/uuid%3A d6605869-37e0-49a6-8bc4-817855ab3710/

[4] S. Hay, R. Mittra, and N. Huang. (2010) Analysis of reflector and feed scattering and coupling effects on the sensitivity of phased array feeds. [Online]. Available: http://csas.ee.byu.edu/docs/Workshop/BYU SGH.pdf

[5] M. Ivashina. (2008) Dutch FPA progress – characterization of efficiency, system noise temperature and sensitivity of focal plane arrays. [Online]. Available: http://ska2008.ivec.org/www/Marianna_Ivashina.pdf

[6] W. A. van Cappellen and L. Bakker. (2010) Eliminating sensitivity ripples in prime focus reflectors with low-scattering phased array feeds. [Online]. Available: http://csas.ee.byu.edu/docs/Workshop/BYU_StandingWaves_Cappellen.pdf

[7] S. N. Makarov, *Antenna and EM Modeling With MATLAB*. New York: John Wiley and Sons, Inc., 2002.

[8] M. V. Ivashina, R. Maaskant, and B. Woestenburg, "Equivalent system representation to model the beam sensitivity of receiving antenna arrays," *IEEE Antennas Wireless Propag. Lett.*, vol. 7, no. 1, pp. 733–737, Jan. 2008.